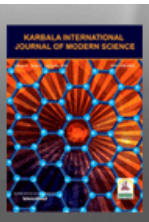
Karbala International Journal of Modern Science

Manuscript 3432

Effect of Au nanoparticles doping on the structure, surface morphology and optical properties of ZnAgO Nanorods

Mohsin Talib Mohammed

Salah M. Saleh Al-Khazali

Bassam A. Salih

Adel H. Omran Alkhayatt

Effect of Au nanoparticles doping on the structure, surface morphology and optical properties of ZnAgO Nanorods

Abstract

In this work, nanoparticles (NPs) composed of noble elements (Au and Ag) were prepared using a chemical reduction method and then combined with a spray pyrolysis technique for synthesizing ZnAgO and Au-doped ZnAgO nanorods (NRs). The films were produced by adding 2 wt% of Ag NPs and 2, 4, and 6 wt% of Au NPs at 420°C. The results showed that the films have a polycrystalline ZnO (wurtzite) with a hexagonal structure. Also, all films had a preference orientation along the (002) plane. The crystal size increased with increasing Au doping from 64.4 to 65.33 nm. For ZnO doped with Ag NPs, a uniform distribution of NPs on the substrate surface with little porosity was observed. After adding Au NPs, there is a variety in the diameter and porosity of the prepared nanorod samples. The diameters range decreased from (180-200) nm for the ZnAgO to (80-120) nm after 2 wt% Au doping and then rose to (190-200) nm and (160-220) nm with 4 wt% and 6 wt% Au doping, respectively. With doping Au at different ratios, the films showed an intense absorbance in the UV extent and great transmittance in the visible area. The optical energy band gap of $ZnAg_xO$ increased from 3.25 eV to 3.35 and 3.32 eV with Au doping of 2 and 4 wt%, respectively, and decreased after adding 6 wt% of Au NPs to 3.26 eV. According to the obtained findings, Au and Ag doping substantially impacted the optical performance of ZnO film

Keywords

Au nanoparticles; Nanorods; Optical properties; Spray pyrolysis; ZnO

RESEARCH PAPER

Effect of Au Nanoparticles Doping on the Structure, Surface Morphology and Optical Properties of ZnAgO Nanorods

Mohsin T. Mohammed [a,*], Salah M. Saleh Al-Khazali [b], Bassam A. Salih [c], Adel H. Omran Alkhayatt [d]

[a] Nanotechnology and Advanced Materials Research Centre, University of Technology, Baghdad, Iraq
[b] The General in Directorate of Education in Al-Najaf Al-Ashraf, Ministry of Education, Al Najaf, Iraq
[c] Electrical Engineering Department, Faculty of Engineering, University of Kufa, Al Najaf, Iraq
[d] College of Medicine, University of Alkafeel, Al Najaf, Iraq

Abstract

In this work, nanoparticles (NPs) composed of noble elements (Au and Ag) were prepared using a chemical reduction method and then combined with a spray pyrolysis technique for synthesizing ZnAgO and Au-doped ZnAgO nanorods (NRs). The films were produced by adding 2 wt% of Ag NPs and 2, 4, and 6 wt% of Au NPs at 420 °C. The results showed that the films have a polycrystalline ZnO (wurtzite) with a hexagonal structure. Also, all films had a preference orientation along the (002) plane. The crystal size increased with increasing Au doping from 64.4 to 65.33 nm. For ZnO doped with Ag NPs, a uniform distribution of NPs on the substrate surface with little porosity was observed. After adding Au NPs, there is a variety in the diameter and porosity of the prepared nanorod samples. The diameters range decreased from (180-200) nm for the ZnAgO to (80-120) nm after 2 wt% Au doping and then rose to (190-200) nm and (160-220) nm with 4 wt% and 6 wt% Au doping, respectively. With doping Au at different ratios, the films showed an intense absorbance in the UV extent and great transmittance in the visible area. The optical energy band gap of $ZnAg_xO$ increased from 3.25 eV to 3.35 and 3.32 eV with Au doping of 2 and 4 wt%, respectively, and decreased after adding 6 wt % of Au NPs to 3.26 eV. According to the obtained findings, Au and Ag doping substantially impacted the optical performance of ZnO film.

Keywords: Au nanoparticles, Nanorods, Optical properties, Spray pyrolysis, ZnO

1. Introduction

Zinc oxide (ZnO) is one of the third-generation wide band gap semiconductor materials that have attracted great interest in the field of electronic functional materials [1]. This is due to its excellent physical and chemical properties, like wide direct band gap energy, facile preparation, and low cost. ZnO NPs have been found to have novel and improved structural, optical, electrical, and chemical properties compared to bulk ZnO materials [2,3]. As a result, many different approaches have been developed for producing ZnO NPs, including hydrothermal, sol-gel, co-precipitation, combustion, high-temperature pyrolysis, and spray pyrolysis [3]. An efficient technique that can alter the electronic structure and improve electrical and optical properties is doping impurity elements into the target lattice [4]. The performance of ZnO has been enhanced by adding several elements as donors, such as Ag, Mg, Al, and Au [5,6]. Many researches and investigations have studied the effect of doping on the characteristics of doped ZnO NPs. Saleem *et al.* synthesized Au- and Sm-doped ZnO films in order to serve as photoanodes for improving the

Received 19 April 2025; revised 28 August 2025; accepted 31 August 2025.
Available online 22 October 2025

* Corresponding author.
E-mail address: mohsint.t.mohammed@uotechnology.edu.iq (M.T. Mohammed).

https://doi.org/10.33640/2405-609X.3432

efficiency of DSSCs. The results revealed that the particle size increases with increasing Au concentration. Also, transmission spectra decreased due to the effect of roughness and porous surface, whereas absorbance increased as the NPs are small and big in the visible light area [4]. Ouarez *et al.* [7] produced ZnO films by doping them with Au using the sol-gel technique at varying Au concentrations. The results demonstrated that the crystal quality of the films reduces with increasing Au concentration. Moreover, both the morphology and roughness were influenced by Au concentration. The high amount of Au concentration in ZnO films led to improvement their transparency, along with an increase in all visible emissions. As is well known, pyrolysis deposition is a straightforward approach that does not necessitate high-quality substrates. It is suited ideally for coating on a large surface, as it can be performed in a non-vacuum system [8,9]. Despite extensive research on elemental doping in ZnO, the effect of Ag-Au co-doping is rarely studied. In this work, the Au and Ag NPs were hybrid synthesized and prepared using a chemical reduction method and combined with a spray pyrolysis technique for the synthesis of ZnAgO NRs and Au-doped ZnAgO. The influence of Au and Ag doping on the structural, morphological, and optical properties of ZnO was also investigated. Compared to previous studies, this work opens new avenues for the rational design and scalable production of complex multi-functional metal oxide nanostructures for advanced applications.

2. Materials and Methods

2.1. Synthesis of Au and Ag NPs

In the current study, Au and Ag NPs were prepared by the chemical reduction method. Gold (III) chloride hydrate ($HAuCl_4.H_2O$, 99% purity), silver nitrate ($AgNO_3$, 99% purity) at a concentration of 0.0005 m, and 1% of sodium citrate (98% purity) were diluted in 100 ml of deionized water in order to control the ratio of these materials with their respective weights. Afterward, 10 ml of $HAuCl_4.H_2O$ or $AgNO_3$ solution was heated to the boiling point, and then a solution of sodium citrate (0.2 ml) was added. The solution was under stirring for 15 min using a magnetic stirrer at room temperature to ensure a complete response. The mechanism of reaction could be expressed as follows [10,11]:

$$2HAuCl_4 + 4Na_3C_6H_5O_7 \rightarrow H_2 + 2Au^0 + 4CO_2 + 4NaC_5H_5O_5 + 8NaCl \quad (1)$$

$$4AgNO_3 + C_6H_5O_7Na_3 + 2H_2O \rightarrow 4Ag^0 + C_6H_5O_7H_3 + 3Na^+ + H^+ + O_2\uparrow \quad (2)$$

2.2. Preparation of ZnAgO and Au-doped ZnAgO nanorods

Ag-doped ZnO NRs and Au-doped ZnAgO NRs were synthesized and coated on glass substrates (3×2 cm^2) using a spray pyrolysis technique at 420 °C. Zinc chloride heptahydrate ($ZnCl_2$) was used as the Zn source. The starting materials were magnetically stirred for 12 min in order to mix the ingredients together and dissolve them completely in deionized water. The prepared Au and Ag NRs solutions were mixed by a chemical reduction method [10,11] and then mixed with ($ZnCl_2$) solution. The substrates were ultrasonically cleaned in distilled water and cleaning powder for 10 min and then put in the beaker containing alcohol with rising purity (12 min) to remove any stuck oil. The optimal circumstances for the deposition parameters were maintained throughout the process. These parameters included 31 cm of the substrate spray nozzle distance, 23 s of spray time, 3 min of spray interval, 50 kg/cm^2 of carrier gas pressure, and 7.5 ml/min of the flow rate. Table 1 shows the weight percent of chemicals used to fabricate ZnAgO NRs with different Au-doped concentrations. The temperature of the substrate was controlled utilizing an iron-constantan thermocouple.

The crystal lattice of samples was investigated by XRD automatic diffractometer (XPert Pro MPD) using Cu: Kα radiations ($\lambda_{K\alpha} = 1.5406$ Å). A scanning electron microscope (SEM) (INSPECT-S50) with an attached EDX system was also utilized at 15 keV to investigate the microstructure of the produced films. At room temperature, the transmittance spectra and optical absorption were recorded from 300 to 800 nm wavelength using a UV spectrophotometer (Model MEGA-2100). The major steps used for preparation and synthesis of Au-doped ZnAgO NRs is shown in Fig. 1.

Table 1. The weight percent of chemicals used for producing ZnAgO NRs with different Au-doped concentrations.

Sample	ZnO (wt %)	Ag (wt %)	Au (wt %)
Z_1	0.98	0.02	0
Z_2	0.96	0.02	0.02
Z_3	0.94	0.02	0.04
Z_4	0.92	0.02	0.06

3. Results and Discussion

3.1. Structural characteristics

Fig. 2 displays the XRD patterns of all produced films. As can be seen from this figure, based on JCPDS card # 36–1451, a hexagonal wurtzite phase of ZnO was detected, and no extra diffraction peaks were found.

The small quantity of Ag^{+}/Au^{+} ions in the ZnO lattice may cause an absence of distinctive peaks associated with Ag and Au [6]. This confirms that Ag^{+}/Au^{+} ions have been uniformly substituted with Zn^{2+} ions or incorporated into the amorphous areas of the ZnO crystal lattice. The peak intensity (002) was measured to explore the influence of doping compounds on the crystallinity of ZnO film. As the amount of Au NPs increased, the intensity of the peak decreased. It was reported that the formation of Zn-Au/Ag imperfections or the isolation of Ag/Au at the grain boundaries could be induced [4,12]; this leads to a drop in the strength of the diffraction peak, which in turn signals a decline in crystal quality. In addition, the intense peaks moved in a slightly upward direction toward 2θ values. The full width at half maximum (FWHM) of these peaks was also expanded for all samples (Z_1, Z_2, Z_3, and Z_4), as shown in Table 2. The peaks were displaced to higher 2θ values as the ionic radii of Au^{+} (1.37 Å) and Ag^{+} (1.15 Å) are greater than Zn^{2+} (0.74 Å) [13]. This doping results in internal stresses; similar effects have been reported by Refs. [4,14]. Table 2 shows the calculated lattice parameters, i.e., a, c, d, and FWHM, which agree with JCPDS Card # 36–1451. From the XRD data, the structural characteristics were determined, such as the lattice constant, the average

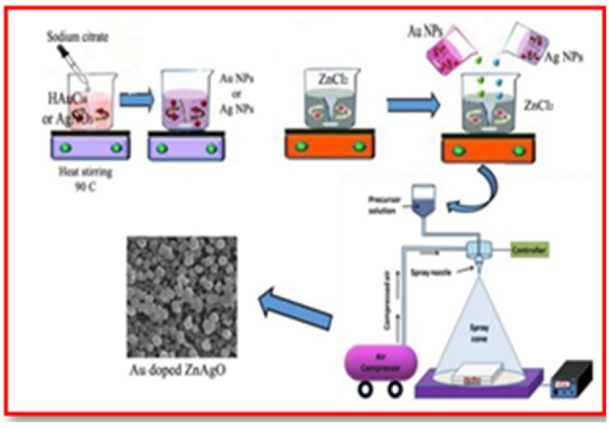

Fig. 1. Schematic illustration of main steps used for preparation and synthesis Au-doped ZnAgO NRs.

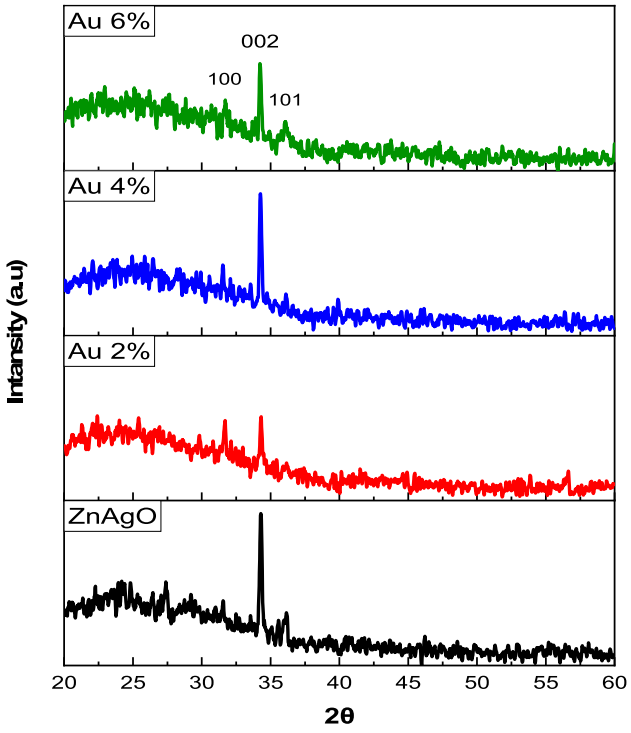

Fig. 2. XRD patterns of pure ZnAgO and Au-doped ZnAgO NRs at various Au concentrations.

crystallite size (D), and the strain (Ɛ). The Scherrer formula was used to determine the crystallite size for the preferred orientations of the produced films [1]:

$$D = \frac{0.9\lambda}{(FWHM)\ COS\ \theta} \tag{3}$$

Where θ is the Bragg angle, and λ is the wavelength 1.5406 Å. Also, Table 2 displays the deviation of the crystallite size as a function of the amount of doped Au NPs. The crystallite size for the (002) plane reduced from 64.2 nm (Z_1) to 50.6 nm (Z_2) and increased to 65.33 nm and 65.01 nm for Z_3 and Z_4, respectively. This clearly indicates that the doping of Ag and Au NPs has contributed significantly to this crystalline change and the samples' preferred growth orientation. Adding dopant atoms (Ag^{+}, and Au^{+}) to the ZnO lattice breaks its periodicity owing to the difference in ionic radius (Ag^{+}: 1.15 Å, Au^{+}: 1.37 Å, and Zn^{2+}: 0.74 Å) or valence. However, this imbalance can cause a strain in the lattice (whether compressive or tensile). Hence, significant strain can impede crystallite formation during synthesis, resulting in different crystallite sizes and lattice parameters [7,14].

The strain (ϵ) has been determined by the following equation [15]:

Table 2. XRD results for pure ZnAgO and Au-doped ZnAgO NRs.

Compound	2 θ	d (Å)	(hkl)	FWHM (deg)	a (Å)	c (Å)	Dislocation Density (δ) 10^{15} Lines/m^2	(N) 10^{16} (m^{-2})	Strain 10^{-3}	Crystallite size (nm)
$Zn_{0.98}Ag_{0.02}O$	31.664	2.8258	(100)	0.3149	3.262	5.233	2.411	1.144	0.0771	64.4
	34.268	2.6168	(002)	0.0984						
	36.176	2.4831	(101)	0.0984						
$Zn_{0.96}Ag_{0.02}Au_{0.02}O$	31.719	2.8210	(100)	0.2362	3.257	5.239	3.905	1.348	0.0768	50.6
	34.226	2.6199	(002)	0.0787						
	36.011	2.4935	(101)	0.6298						
$Zn_{0.94}Ag_{0.02}Au_{0.04}O$	31.668	2.8255	(100)	0.0984	3.262	5.232	2.366	1.675	0.0780	65.33
	34.278	2.6161	(002)	0.1378						
	36.073	2.4899	(101)	0.1574						
$Zn_{0.92}Ag_{0.02}Au_{0.06}O$	31.534	2.8372	(100)	0.1181	3.276	5.236	2.343	1.091	0.0773	65.01
	34.247	2.6184	(002)	0.0984						
	38.298	2.3502	(101)	0.1968						

$$\text{Strain}\ (\epsilon) = \frac{|C_{JCPDS} - C_{XRD}|}{C_{JCPDS}} \times 100\% \quad (4)$$

The deviation of strain ($\mathcal{E}$) as a function of the content of Au-doped ZnAgO NRs for (002) planes is shown in Fig. 3. It can be noticed that the strain increases with increasing Au NPs amount up to 2 and 4 wt%, then it decreases after adding 6 wt%. The crystallization process in polycrystalline thin films is responsible for micro-strain changes. Crystallization under doping (Ag^+, and Au^+) introduces atomic-scale distortions like lattice mismatch and defects that display as a strain and become "locked in" during the rapid synthesis spray pyrolysis method [16,17].

3.2. Morphological properties

Fig. 4 (a–h) demonstrates the SEM images and particle size distributions of the ZnAgO and Au-

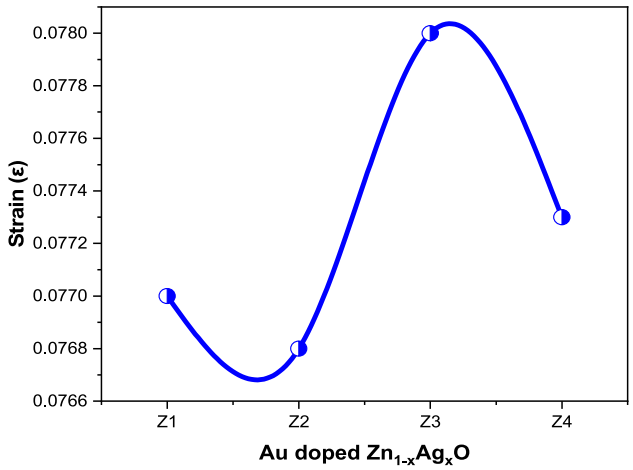

*Fig. 3. The deviation of strain (ϵ) as a function of Au-doped ZnAgO content for (**002**) plane.*

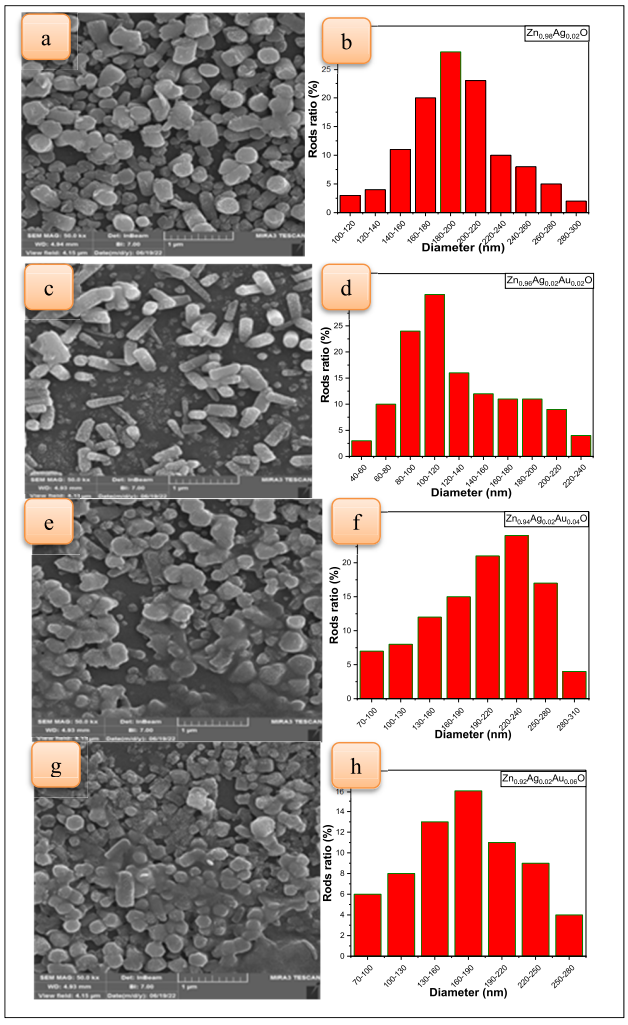

Fig. 4. Surface morphology of ZnAgO and Au doped ZnAgO obtained from SEM images analysis and the histogram distribution of the diameters: (a, b) ZnAgO, (c, d) 2 wt% Au, (e, f) 4 wt% Au, and (g, h) 6 wt % Au.

doped ZnAgO NRs. For ZnAgO (sample Z_1), a vertical growth on the substrate surface with a hexagonal structure in the diameter range of (180–200) nm can be observed along with a homogeneous distribution morphology (Fig. 4 (a, b)). This phenomenon indicates that Ag NPs promoted the crystallization of ZnO NRs. This result agrees with the literature [18,19]. The presence of small spherical shapes (dated back to the Au NPs), a large porosity between the NRs, and a small diameter size of NRs (80-120 nm) were displayed when 2 wt% of Au NPs was added (sample Z_2) (see Fig. 4 (c, d)). In the case of the high content of Au NPs (4 and 6 wt%) (Fig. 4(e–h)), the coalescence was highly improved so that the inter-cluster porosity disappeared and the diameter of NRs was enhanced slightly to (190-240) nm and (160-220) nm in samples Z_3 and Z_4, respectively. At low doping (2 wt%), Au NPs poison lateral growth by pinning surface diffusion of ZnO, which may decrease NR diameter. However, after high doping (4 and 6 wt%), Au NPs coalesce during high-temperature synthesis, which could form liquid bridges. This promotes ripening and NR merging, along with larger diameters [20]. It appears that the addition of Au NPs is the main reason for these observed variations in the nanostructure of the samples. The elemental composition of all Au-doped ZnAgO NRs films was provided by the EDS analysis, as shown in Fig. 5. It can be noted that all peaks resulting from the EDS analysis confirm the chemical compositions planned in this study, as the weight percentages of Au NPs increase successively in a noticeable manner with the increase in the percentages of Au added to the investigated samples. Also, peaks of undesirable additional elements were not detected. The EDS spectra for all samples indicated that the greatest peak is related to the Zn concentration. At 2 wt% Au doping, the peak diminished, then increased again at 4 and 6 wt% Au doping. This result aligns with the XRD observation and proves that noble metals are incorporated consistently into the ZnO. Furthermore, it signifies that Ag and Au atoms replace Zn atoms inside the lattice structure of ZnO.

3.3. Optical properties

Fig. 6 displays the absorbance spectrum as a function of wavelength for Au-doped ZnAgO NRs in various concentrations of Au NPs. For sample Z_1, a high absorption edge at 378.5 nm was noticed, which may be associated with the wurtzite structure of ZnO. This is due to the movement of electrons from the semiconductor's valence band to its conduction band after absorbing light [21]. The

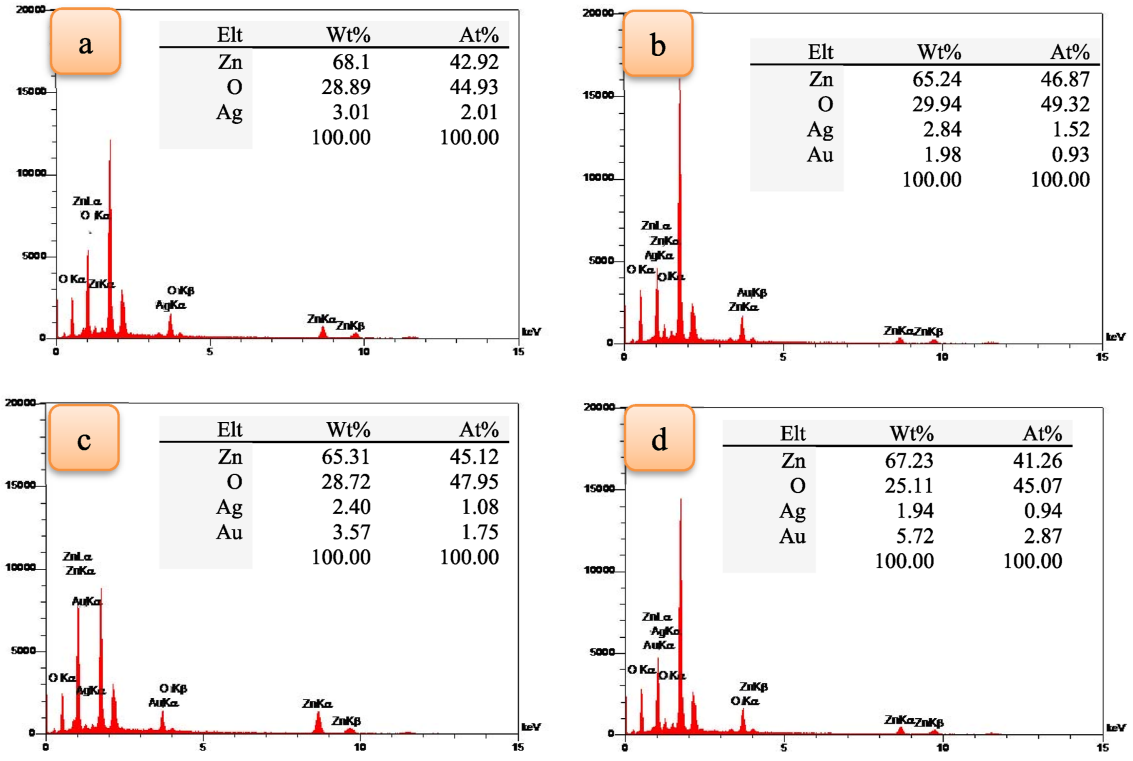

Fig. 5. EDS spectrum of ZnAgO with different Au concentrations: (a) 0 wt% Au, (b) 2 wt% Au, (c) 4 wt% Au, and (d) 6 wt% Au.

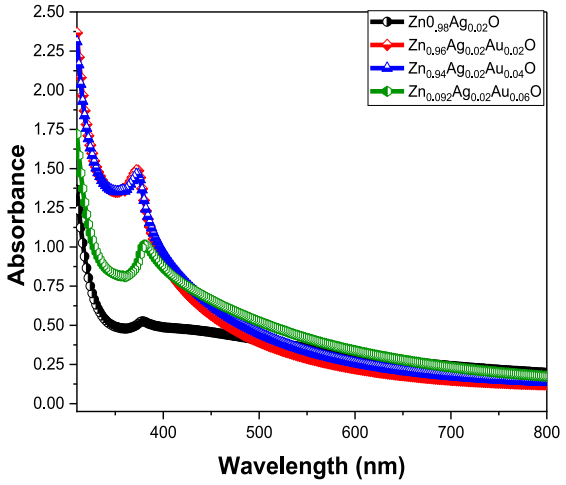

Fig. 6. The absorbance as a function of incident wavelength for pure ZnAgO and Au-doped ZnAgO NRs.

absorption edge values of the Z_2, Z_3, and Z_4 samples were 372, 373, and 383 nm, respectively. For all samples, the absorption edge is very sharp and lies in the ultraviolet range. Compared to sample Z_1, the optical absorption edge for Z_2 and Z_3 samples was shifted towards the small wavelengths, signifying a rise in the band gap. Here, adding Au and Ag NPs to ZnO NRs generally enhanced the absorbance intensity. Fig. 6 also exhibited that the absorbance of Au-doped ZnAgO is greater than that of ZnAgO. This suggests the possibility of using the Au-doped ZnAgO as a UV blocking agent in sunscreens.

Fig. 7 illustrates the transmittance spectra of the ZnAgO and Au-doped ZnAgO NRs for three different Au concentrations. The results showed a very transparent zone at (390-800) nm, with an average transmission value of around (65-76)%, which agrees with the literature [4,8] and is close to the average values for Nb_2O_5:WO_3 [22]. Recent studies [6,8] pointed out that the increased grain size and porosity of the ZnO NRs doped with Au NPs may be responsible for the observed improvement in optical transparency. The SEM results (Fig. 3) seem to back up this pattern of increasing transmittance. The optical band gaps (Eg) of all films were estimated from TAUC plots, using Eq. 5 [1,3]:

$$\alpha h\upsilon = A\left(h\upsilon - E_g\right)^n \quad (5)$$

Where α is the absorption coefficient, hv is the photon energy, h is the Planck's constant, A is a constant, and n is a value dependent on the type of transition (n = 1/2; direct in this case).

The plots of $(\alpha h\upsilon)^2$ vs. hν for ZnAgO NRs and Au-doped ZnAgO NRs at diverse amounts of Au NPs are displayed in Fig. 8, where the band gap of the Z_1 sample is found to be 3.28 eV. This value is quite like the one reported by Ref. [9]. After increasing Au concentration for samples (Z_2 and Z_3), Eg values were increased to 3.35 and 3.32 eV, respectively. This is probably due to the Burstein-Moss effect [6]. It was reported that the increase in the amount of Au NPs may lead to the band gap widening [8,23]. However, the energy band gap decreased with increasing the content of Au NPs to 6 wt% (Z_4 sample). This consequence is consistent with the results obtained from XRD measurements.

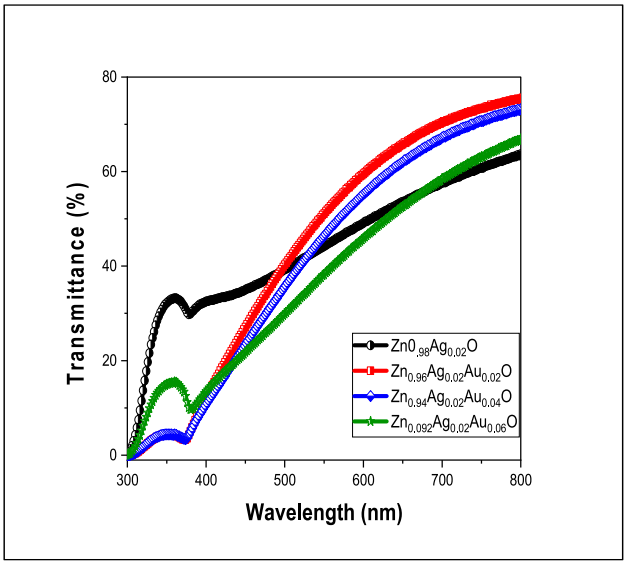

Fig. 7. The transmittance as a function of incident wavelength for pure ZnAgO and Au-doped ZnAgO NRs.

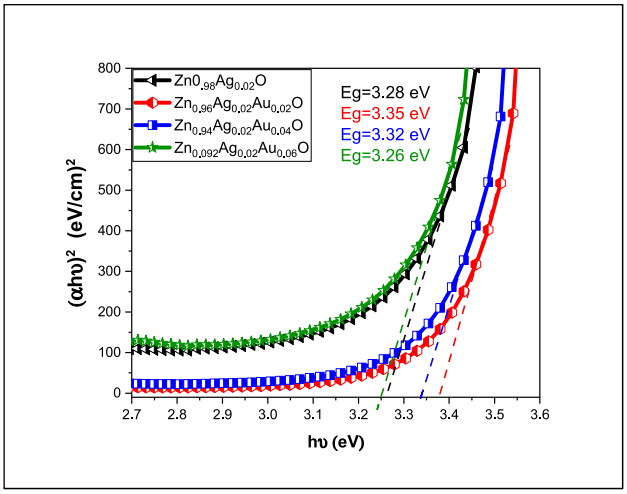

Fig. 8. The plots of $(\alpha h\upsilon)^2$ vs. hν of ZnAgO NRs doped with different concentrations of Au NPs.

The sample Z_4 has a larger average crystallite size than ZnAgO (Z_1 sample). This can be attributed to the rise of defects such as impurities or incomplete dopant substitution with the host atoms. These results are consistent with previous research [4,24]. Ag and Au NPs significantly affect the fabrication mechanism of ZnO NRs, which in turn determines the optical and structural nanoscale properties. This confirms the importance of ZnO nanorods' rational synthesis for their full potential in fundamental studies and single nanorod electronic devices.

4. Conclusions

In this work, Ag and Au NPs were prepared by the chemical reduction process, and the products were successfully combined with ZnO solutions by the chemical spray pyrolysis method to prepare ZnAgO and Au-doped ZnAgO NRs in different amounts of Au NPs at 420 °C. The main conclusions can be summarized as follows:

- XRD data disclosed that all fabricated samples have a polycrystalline structure and a good crystalline nature. The crystallite size for the preferred orientation (002) increased from 64.4 nm to 65.01 nm with increasing Au NP doping level.
- An increase in micro-strain was obtained with increasing Au NPs content. The low micro-strain values showed that the spray pyrolysis acts well as a method for depositing high-quality Au-doped ZnAgO NRs.
- The obtained films had noted variations in the nanostructure with a homogeneous distribution morphology by co-doping Au and Ag NPs.
- The investigation of optical properties exhibited that the produced films have great transmittance (over 75%) in the visible spectrum and high absorbance in the UV spectrum.
- The optical energy gap values for direct allowed transitions were shifted from 3.28 eV to 3.32 eV when Au NPs doping content increased from 2 wt% to 4 wt%. However, the energy gap decreased to 3.26 eV after Au doping with 6 wt% Au NPs.

Ethical information

This study does not involve any human participants or animal experiments requiring ethical approval.

Funding

No external funding received.

Conflict of interest

The authors declare that they have no conflicts of interest.

Acknowledgments

The authors would like to sincerely thank the Faculty of Engineering and Faculty of Science, University of Kufa, Iraq, for supporting them during the research.

References

[1] H.S. Al-Salman, M.J. Abdullah, Fabrication and characterization of undoped and cobalt-doped ZnO based UV photodetector prepared by RF-sputtering, Mater. Sci. Technol. 29 (12) (2013) 1139–1145, https://doi.org/10.1016/j.jmst.2013.10.007.

[2] J.M. Tuama, M.F. Alias, Synthesis of ZnO: ZrO_2 nanocomposites using green method for medical applications, Karbala Intern. J. Modern Sci. 10 (3) (2024) 418–430, https://doi.org/10.33640/2405-609X.3366.

[3] A. Alasmari, A.A. Awad, A.A. Aboud, Investigating the influence of yttrium doping on physical properties of ZnO thin films deposited via spray pyrolysis, Opt. Mater. 148 (114899) (2024) 1–11, https://doi.org/10.1016/j.optmat.2024.114899.

[4] M. Saleem, K. Irshad, S.U. Rehman, M.S. Javed, M. A. Hasan, H.A. Ali, M.Z. Malik, S. Islam, Characteristics and photovoltaic applications of Au-doped ZnO-Sm nanoparticle films, Nanomaterials 11 (702) (2021) 1–14, https://doi.org/10.3390/nano11030702.

[5] B.G. Shohany, A.K. Zak, Doped ZnO nanostructures with selected elements - structural, morphology and optical properties: a review, Ceram. Int. 46 (5) (2019) 5507–5520, https://doi.org/10.1016/j.ceramint.2019.11.051.

[6] M.A. Saidani, A. Fkiri, L.S. Smiri, Copper-doped hybrid Agx–Auy@ZnO nanoparticles and their enhanced photocatalytic activities, J. Inorg. Organomet. Polym. Mater. 29 (2019) 1130–1140, https://doi.org/10.1007/s10904-019-01075-6.

[7] L. Ouarez, A. Chelouche, T. Touam, R. Mahiou, D. Djouadi, A. Potdevin, Au-doped ZnO sol-gel thin films: an experimental investigation on physical and photoluminescence properties, J. Lumin. 203 (2018) 222–229, https://doi.org/10.1016/j.jlumin.2018.06.049.

[8] A. Bhosale, J. Kadam, T. Gade, K. Sonawane, K. Garadkar, Efficient photodegradation of methyl orange and bactericidal activity of Ag doped ZnO nanoparticles, J. Indian Chem. Soc. 100 (100920) (2023) 1–12, https://doi.org/10.1016/j.jics.2023.100920.

[9] A.H. Husien, G. Tseberlidis, V. Trifiletti, E. Fabbretti, S. Mostoni, J. McGettrick, T. Watson, R. Po, S. Binetti, Optimized hot injection and HCl purification for high quality Cu_2ZnSnS_4 nanoparticles, Nanoscale Adv. 7 (1) (2025) 250–260, https://doi.org/10.1039/d4na00843j.

[10] L. Mulfinger, S.D. Solomon, M. Bahadory, A. V. Jeyarajasingam, S.A. Rutkowsky, C. Boritz, Synthesis and study of silver nanoparticles, J. Chem. Educ. 84 (322) (2007) 1–4, https://doi.org/10.1021/ed084p322. .

[11] J. Kimling, M. Maier, B. Okenve, V. Kotaidis, H. Ballot, A. Plech, Turkevich method for gold nanoparticle synthesis revisited, J. Phys. Chem. B 110 (32) (2006) 15700–15707, https://doi.org/10.1021/jp061667w.

[12] B. Houng, C.J. Huang, Structure and properties of Ag embedded aluminum doped ZnO nanocomposite thin films prepared through a sol–gel process, Surf. Coat. Technol.

201 (6) (2006) 3188–3192, https://doi.org/10.1016/j.surfcoat.2006.06.043.
[13] N. Güy M. Özacar, The influence of noble metals on photocatalytic activity of ZnO for Congo red degradation, Int. J. Hydrogen Energy 41 (44) (2016) 20100–20112, https://doi.org/10.1016/j.ijhydene.2016.07.063.
[14] U. Chaitra, A.V. Muhammed Ali, M.G. Mahesha, A. Kompa, D. Kekuda, K. Mohan Rao, Property evaluation of spin coated Al doped ZnO thin films and Au/AZO/FTO Schottky diodes, Super, Lattices Microstruct. 155 (106903) (2021) 1–10, https://doi.org/10.1016/j.spmi.2021.106903.
[15] O. Kenan, Strain-induced photoresponsivity in gallium-doped ZnO thin film based UV photodetectors, Sensor Actuator Phys. 366 (114953) (2024) 1–6, https://doi.org/10.1016/j.sna.2023.114953.
[16] C.H. Hsueh, Evaluation of interfacial properties of fiber-reinforced ceramic composites using a mechanical properties microprobe, J. Am. Ceram. Soc. 76 (12) (1993) 3041–3050, https://doi.org/10.1111/j.1151-2916.1993.tb06607.x.
[17] A. Janotti, C.G. Van de Walle, Fundamentals of zinc oxide as a semiconductor, Rep. Prog. Phys. 72 (126501) (2009) 1–29, https://doi.org/10.1088/0034-4885/72/12/126501.
[18] E.D. Fakhrutdinova, A.V. Volokitina, S.A. Kulinich, D. A. Goncharova, T.S. Kharlamova, V.A. Svetlichnyi, Plasmonic nanocomposites of ZnO-Ag produced by laser ablation and their photocatalytic destruction of rhodamine, tetracycline and phenol, Materials 17 (527) (2024) 1–20, https://doi.org/10.3390/ma17020527.
[19] S. Soylu, M. Kara, M. Türkmen, B. Şahin, Synergistic effect of foeniculum vulgare essential oil on the antibacterial activities of Ag-and Cu-substituted ZnO nanorods (ZnO-NRs) against food, human and plant pathogenic bacterial disease agents, Inorg. Chem. Commun. 146 (110103) (2022) 1–10, https://doi.org/10.1016/j.inoche.2022.110103.
[20] R.M. German, Sintering: from Empirical Observations to Scientific Principles, first ed., Butterworth-Heinemann, Oxford. 2014 https://doi.org/10.1016/C2012-0-00717-X.
[21] D. Sahu, N.R. Panda, B.S. Acharya, A.K. Panda, Enhanced UV absorbance and photoluminescence properties of ultrasound assisted synthesized gold doped ZnO nanorods, Opt. Mater. 36 (8) (2014) 1402–1407, https://doi.org/10.1016/j.optmat.2014.03.041.
[22] P. Chaiworn, W. Teerananattapong, P. Reunchan, A. Tubtimtae, E. Wongrat, Effect of tungsten oxide concentration on structural, morphological, compositional, dispersion energy, and linear/nonlinear optical properties of niobium pentoxide thin films, Opt. Mater. 161 (116807) (2025) 1–20, https://doi.org/10.1016/j.optmat.2025.116807.
[23] F.A. Rahman, K.L. Foo, Synthesis and characterization of gold doped zinc oxide nanostructure for biosensor application, AIP Conf. Proc. 1892 (2017) 020024, https://doi.org/10.1063/1.5005655.
[24] A. Fatehmulla, B.A. Shamsan, A.M. El-Naggar, A. M. Aldhafiri, N. Qureshi, T. Kim, M. Atif, A. Mahmood, M. Asif, Physical characteristics, blue-green band emission and photocatalytic activity of Au-decorated ZnO quantum dots-based thick films prepared using the doctor blade technique, Molecules 28 (4644) (2023) 1–20, https://doi.org/10.3390/molecules28124644.